Proceedings of the ASME 2023
5th International Offshore Wind Technical Conference
IOWTC2023
December 18-19, 2023, Exeter, United Kingdom

IOWTC2023-119374

MOORING FORCE ESTIMATION FOR FLOATING OFFSHORE WIND TURBINES WITH AUGMENTED KALMAN FILTER: A STEP TOWARDS DIGITAL TWIN

Kobe Hoi-Yin Yung
Department of Naval Architecture, Ocean and Marine Engineering, University of Strathclyde, UK

Qing Xiao
Department of Naval Architecture, Ocean and Marine Engineering, University of Strathclyde, UK

Atilla Incecik
Department of Naval Architecture, Ocean and Marine Engineering, University of Strathclyde, UK

Peter Thompson
Arup Hong Kong, China

ABSTRACT

During the recent research studies Digital Twin (DT) simulation models for Structural Health Monitoring (SHM) based on data-driven mode have been developed, which can provide accurate simulation and prediction of mooring forces of Floating Offshore Wind Turbines (FOWTs). However, the performance of this kind modelling is highly affected by the quantity of real data training set and it is limited to some specific configuration and the recorded environmental conditions. More importantly, the data-driven DT cannot interpret the physical meaning of structural dynamic interactions.

Therefore, a new Physics-Based estimator is proposed in this work. The fully coupled FOWT simulations are carried out in QBlade Ocean and the simulation results are used to prepare the Reduced-Order Model by system identification for different sea states. The proposed estimator is based on the Augmented Kalman Filter in which the unknown mooring force is augmented as a state. The prediction of state is adjusted with the measurable platform motion data. It demonstrates the ability of filtering the noise in measurements and capturing the dynamic behaviour of FOWT with acceptable low computational cost. This real-time state estimator also provides the foundation of developing the DT modelling framework of FOWT and enables us to scale-up FOWTs in the next stage.

Keywords: Digital Twin, Floating offshore wind turbine (FOWT), Mooring

1. INTRODUCTION

Offshore wind energy demonstrated as reliable energy source over the past decade and contributed to the road of decarbonisation. There was 48.2 GW offshore wind capacity already completed by 2021 [1]. Particularly, the Floating Offshore Wind Turbines (FOWTs) have received great attention recently, and it is expected to have higher potential to harvest wind energy than traditional fix-bottom type offshore wind turbines. In terms of the structural integrity and operational requirements, the mooring systems dictate survivability of FOWT under the extreme wave loading and the required station-keeping performance.

The traditional Oil and Gas (O&G) installation Floating Production Storage and Offloading (FPSO) platforms typically has 10 to 30 mooring lines for a unit, whilst a FOWT has fewer redundancy with 3 to 6 mooring lines. And there are about 150-300 mooring lines for a FOWT farm with high cost of Operational Expenditure (OPEX) [2]. Therefore, developing the strategy for structural inspection and maintenance is very critical.

There are different ways to perform structural health monitoring of the mooring system, such as visual inspection by divers and Non-destructive testing with remotely operated vehicles. These methods are considered high risk and costly [3].

Mooring line tension monitoring is effective to track structural health. It can be categorised into direct and indirect methods. Direct method refers to the installation of load cells on the chain and detecting the failure. Figure 1 shows the load pin arrangement installed on Hywind project for monitoring the mooring design load ranged up to 2000 tonnes tension. Yet it has low accuracy [4].

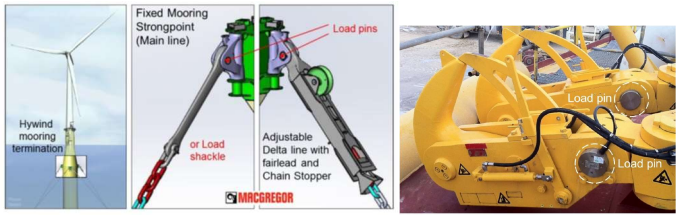

FIGURE 1: MOORING LINE TERMINATION AT THE HULL OF STATOIL'S (NOW EQUINOR) HYWIND SPAR FLOATER. LOAD MONITORING PINS MOUNTED ON MOORING QUICK RELEASE HOOKS FROM MAMPAEY [5]

Using an inclinometer is considered as an indirect method. The tension can be derived from the mooring line angle based on the catenary equations or look-up table.

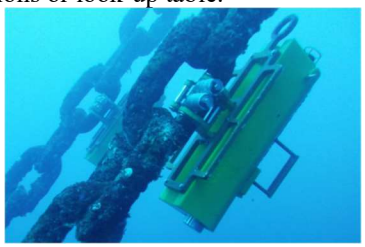

FIGURE 2: INCLINOMETERS INSTALLED ON TOP CHAIN. COURTESY: PULSE [5]

Nevertheless, this method cannot capture the dynamic effects and highly nonlinear behavior. When the line is tightened, there is less variation of inclination angle and less sensitivity of the measurement [5]. Both the load cell and inclinometer are installed underwater which face the problem of fragility under severe wave conditions, and lead to a high OPEX.

An alternative method is to monitor the floating platform position. The monitoring is based on differential navigation systems, such as the Differential Global Positioning System (DGPS), and it can achieve the update rate of 10Hz, the turret's center with respect to reference position [4][5].

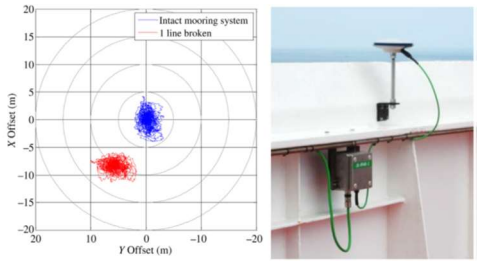

FIGURE 3: (LEFT) VESSEL OFFSET DUE TO A SINGLE BROKEN MOORING LINE. (RIGHT) ANTENNA OF A DGPS MONITORING SYSTEM OUTSIDE THE CONTROL ROOM OF AN FPSO. COURTESY: SOFEC [5]

This system can detect the failure by calibration, but the intention is not to estimate the dynamic loading along the mooring line. A more sophisticated system is required to estimate the internal stress and to predict the fatigue life in order to improve the maintenance and repair strategy. Therefore, DT as a digital representation of real system is used to monitor this critical asset and to predict the future performance.

In developing the DT model, there are mainly two approaches, Data-Driven Model (DDM) and Physical Model (PM). Machine learning (ML) techniques are prevalent nowadays to perform DT, such as Kernel Method [6], Artificial Neural Network [7], Long Short-Term Memory (LSTM) [8], Principle Component Analysis (PCA) [8], etc. By fitting a large amount of data set into Kernel regularized least square algorithms, KM DDM in [6] can accurately calculate the relationship between the input and output spaces with the largest Mean Absolute Error (MAE) 22.9 ± 0.2 kN axial tension of a mooring line bridle, defined by the average absolute distance between the prediction and actual value [9]. However, the performance of DDM deteriorates if the real sea condition is out of the range of the training data set [10] and the geometry or other structural dynamic behaviour varying over time. On the other hand, it is worth noting that developing DT based on PM can provide structural dynamic interpretations and there is no problem of generating the simulations with different environmental loading scenarios when comparing to DDM approach.

One of the methods to build DT based on PM is the Kalman Filter, which is a recursive online algorithm [11]. The theory can be extended for unknown input estimation which is known as Augmented Kalman Filter (AKF) and it has been adopted for load estimation for onshore wind turbines and the effective wind estimation for wind turbines. A recent work demonstrated a DT for a TetraSpar full scale prototype and provided reasonable estimation of tower-based loading [12]. However, this DT only considered one operating point and the dynamic environment of real sea states, which require multiple operating points for system state and control dynamics, may not be fully captured. To the best of authors' understanding, there is no published DT can simultaneously perform load estimation for unmeasurable states (e.g. mooring forces), interpret the physical meaning of the structural dynamics system and can be used in wide spectrum of sea states with low cost of computational time.

Due to the above reasons and the niche of developing true DT, this paper presents a new PM DT prototype with automated algorithm for adapting different sea states.

2. MATERIALS AND METHODS

The prototype DT is developed based on the simulation in QBlade Ocean [13], a well-developed open-source software for calculating the dynamic motions of FOWTs. By considering the hardly measurable instantaneous wave elevation and dynamic mooring loading as the "unmeasurable" and unknown input parameters, the AKF is adopted to estimate the unknown inputs based on only the measurable platform motions simulated in QBlade. The real motions can be acquired with some standard measurements e.g., inclinometer, Motion Reference Unit (MRU) that are readily available in the market. And the multiple sea states adaptive algorithm is developed based on Multiple-Model Adaptive Estimation (MMAE).

2.1 Reduced-Order Model

In this paper, the semi-submersible FOWT DeepCwind OC4 model is carried out in QBlade Ocean. The configuration is depicted in Figure 4 and 5. This study takes into account the mass of blades, nacelle, tower, the substructure floating platform with different wave height and period of regular wave inputs. Aerodynamics load is excluded as explained in the following.

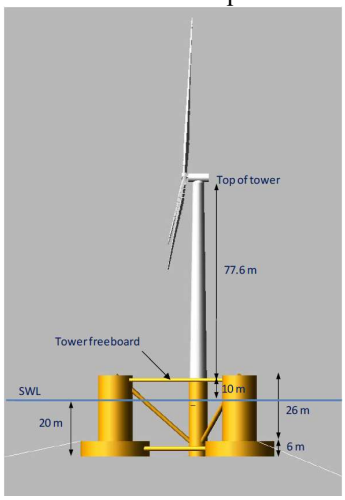

FIGURE 4: DEEPCWIND FLOATING WIND CONFIGURATION [14]

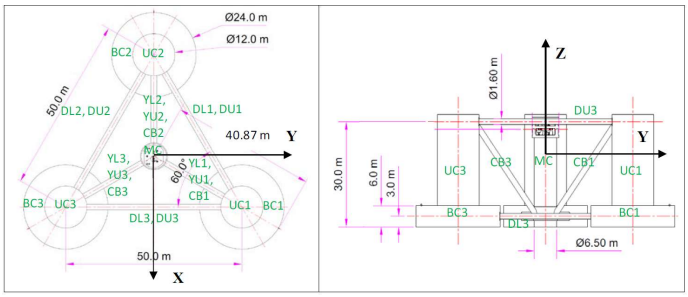

FIGURE 5: PLAN (LEFT) AND SIDE (RIGHT) VIEW OF THE DEEPCWIND SEMISUBMERSIBLE PLATFORM WITH DIMENSIONS [14]

QBlade allows to perform the hydrodynamic loading on floating platform using the combination of potential theory and the Morison equation. More precisely, the submerged cylinder is subdivided into elements for capturing the wave kinematics and elevation at the local instantaneous position of the cylindrical element. The simulation results of QBlade were validated with experimental measurements as shown in the past technical reports [15].

Although the state-of-art QBlade Ocean Community Edition can calculate the complicated coupling of dynamic loading and structural response, the computation time still cannot afford the real-time calculation. The environmental condition setting in each simulation cannot be changed over time and adapt the conditions provided from external sensor data. Hence, the reduced-order model is developed based on the knowledge of the equations of motion.

The equations of motion of FOWT based on Cummin's equation [16] for response $q(t)$ is described as follows,

$$(M + A_\infty)\ddot{q}(t) + \int_{-\infty}^{t} B(t-\tau)\cdot\dot{q}(\tau)\cdot d\tau + C\cdot q(t) = F_{aero} + F_{hydr} + F_{moor} \quad (1)$$

Where M is the mass matrix; A_∞ is the infinite-frequency hydrodynamic added mass matrix; B is the radiation damping and retardation function, which is a convolution term of velocity corresponding to the memory effect of fluid motion; τ is a dummy variable of time, t; C is the hydrostatic stiffness matrix.

According to the equation (1), F_{hyd} wave force term can be described as proportional to the wave elevation $\eta(t)$. F_{moor} is the resultant mooring force to restore the FOWT. F_{aero}, in general, refers to the aerodynamic thrust acting to the wind turbine. In design load analysis, both F_{aero} and F_{hydro} cause the restoring mooring tension while F_{hyd} contributes significantly to the variation of the cycling mooring force. [17] revealed the Elementary Effects Method sensitivity of the mooring fair lead tension due to hydrodynamic and wave parameters is substantially higher than the one due to aerodynamic parameters (with controller strategy embedded) in both ultimate load and fatigue load cases. For considering the operation of mooring in long term and high cycle fatigue problem, the load amplitude variation of cyclic motion is the major concern and therefore only F_{hydro} is considered in this study for simplification. The F_{aero} effect will be considered in the future work. The water current effect is not considered in this study. Thus, the input vectors for deriving the following state-space model are $\eta(t)$ and F_{moor}.

The restoring system of mooring is given below:

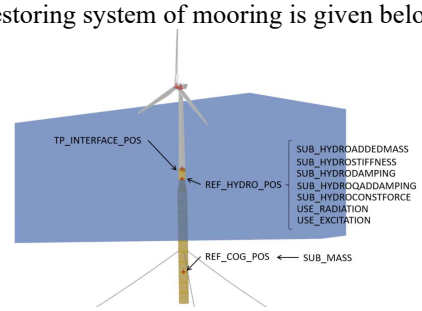

FIGURE 6: DEFINITION OF CENTER OF MASS (CM) IN QBLADE

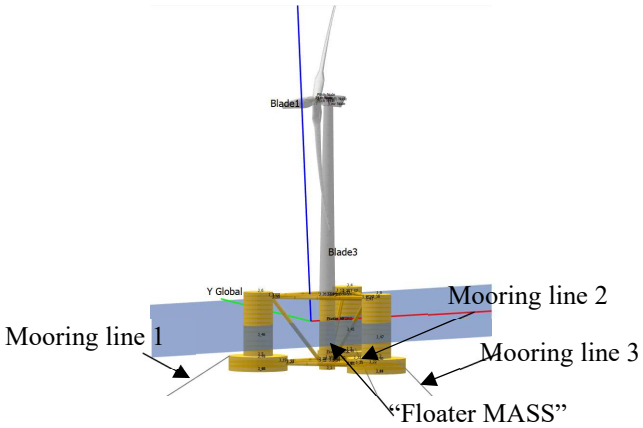

FIGURE 7: CENTER OF MASS (CM) NAMED "FLOATER MASS" FOR OC4 SEMI-SUBMERSIBLE IN QBLADE

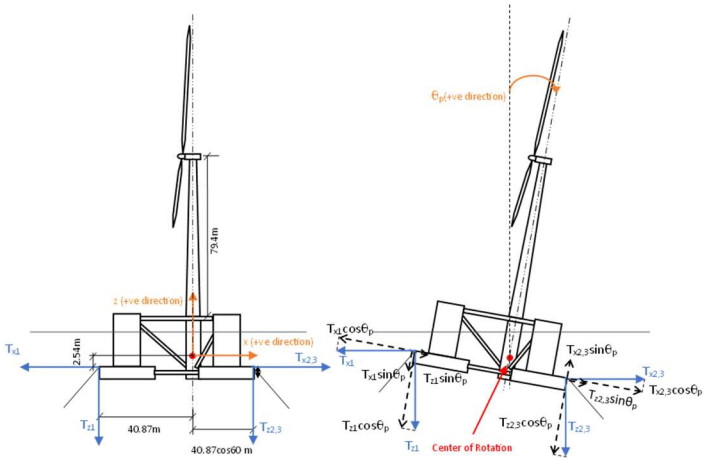

FIGURE 8: RESTORING FORCES AND MOMENTS DUE TO THE MOORING LINE SYSTEM

The pitch angle given in QBlade refers to the center of rotation stated in Figure 8. The mooring force tension output in QBlade are T_{x1}, T_{x2}, T_{x3} in X direction and T_{z1}, T_{z2}, T_{z3} in Z direction for mooring line number 1, 2 and 3 respectively.

The total restoring moments due to mooring force in surge F_{mx}, heave F_{mz} and pitch $F_{m\theta_p}$ are derived below,

$$F_{mx} = T_{x2} + T_{x3} - T_{x1}$$
$$F_{mz} = -T_{z1} - T_{z2} - T_{z3} \quad (2)$$

The center of rotation is assumed to be the center of mass.

$$M_{T1} = (T_{x1}cos\theta_p - T_{z1}sin\theta_p)2.54 - (T_{z1}cos\theta_p + T_{x1}sin\theta_p)40.87$$
$$M_{T2} = -(T_{x2}cos\theta_p + T_{z2}sin\theta_p)2.54 + (T_{z2}cos\theta_p - T_{x2}sin\theta_p)40.87cos60° \quad (3)$$

M_{T3} is derived similarly as M_{T2}.

$$F_{m\theta_p} = M_{T1} + 2M_{T2} \quad (4)$$

Considering the strong coupling relationship between surge x, heave z and pitch θ_p platform motion, a simplified 3-DOF continuous-time state space model is developed based on the system identification using MATLAB Subspace N4SID [18] with the external excitation as the input vectors.

The continuous-time state space model is discretised with time step dt and the process noise $\boldsymbol{W}$ and measurement noise $\boldsymbol{V}$ are introduced to take into account the uncertainties as described in the following,

$$\boldsymbol{X}_k = \boldsymbol{A}_d\boldsymbol{X}_{k-1} + \boldsymbol{B}_d\boldsymbol{u}_{k-1} + \boldsymbol{W}_{k-1}$$
$$\boldsymbol{Y}_k = \boldsymbol{C}_d\boldsymbol{X}_k + \boldsymbol{V}_{k-1} \quad (5)$$

Where the k is the time step, the state vector is $\boldsymbol{X} = [x\ \dot{x}\ z\ \dot{z}\ \theta_p\ \dot{\theta_p}]^T$ and the discrete-time state matrix A_d and input matrix B_d are given by Taylor-series expansion [19]

$$\boldsymbol{A}_d \approx \boldsymbol{I} + \frac{\partial f}{\partial x}dt$$
$$\boldsymbol{B}_d \approx \frac{\partial f}{\partial u}dt \quad (6)$$
$$\boldsymbol{C_d} = \begin{bmatrix} 1 & 0 & 0 & 0 & 0 & 0 \\ 0 & 0 & 1 & 0 & 0 & 0 \\ 0 & 0 & 0 & 0 & 1 & 0 \end{bmatrix}$$

Where the $\boldsymbol{C_d}$ is the output matrix for mapping the internal states to the measurable outputs.

2.2 State Estimation

The unmeasurable parameters vector β to be estimated:

$$\beta = \begin{bmatrix} \eta & F_{mx} & F_{mz} & F_{m\theta_p} \end{bmatrix}^T \quad (7)$$

The augmented states are stated as:

$$\boldsymbol{X}_A = \begin{bmatrix} \boldsymbol{X} \\ \beta \end{bmatrix} \quad (8)$$

The dynamic of unmeasurable parameters via random walk model is considered as following,

$$\beta_k = \beta_{k-1} + W_p \quad (9)$$

Where W_p is the stochastic white noise.

The augmented system matrices are consequently defined as:

$$\boldsymbol{A}_a = \begin{bmatrix} \boldsymbol{A}_d & \boldsymbol{B}_d \\ \boldsymbol{0} & \boldsymbol{D} \end{bmatrix}$$
$$\boldsymbol{C}_a = [\boldsymbol{C}_d \quad \boldsymbol{0}] \quad (10)$$

Where $\boldsymbol{D}$ is the identity matrix and $\boldsymbol{0}$ is the zeros matrix.

The discrete time augmented state space model is derived as,

$$\boldsymbol{X}_{A\,k} = \boldsymbol{A}_a\boldsymbol{X}_{A\,k-1} + \boldsymbol{W}_a$$
$$\boldsymbol{Y}_k = \boldsymbol{C}_a\boldsymbol{X}_{A\,k-1} + \boldsymbol{V} \quad (11)$$

The Kalman Filtering process includes

Prediction

$$\hat{\boldsymbol{X}}_{A\,k}^- = \boldsymbol{0}$$
$$\boldsymbol{P}_k^- = \boldsymbol{A_a}\boldsymbol{P}_{k-1}^+\boldsymbol{A_a}^T + \boldsymbol{Q} \quad (12)$$

Innovation

$$\boldsymbol{y}_k = \boldsymbol{z}_k - \boldsymbol{C}_a\hat{\boldsymbol{X}}_{A\,k}^-$$
$$\boldsymbol{K}_k = \boldsymbol{P}_k^-\boldsymbol{A}_a{}^T\left(\boldsymbol{C}_a\boldsymbol{P}_k^-\boldsymbol{C}_a{}^T + \boldsymbol{R}\right)^{-1}$$
$$\hat{\boldsymbol{X}}_{A\,k}^+ = \hat{\boldsymbol{X}}_{A\,k}^- + \boldsymbol{K}_k\boldsymbol{y}_k$$
$$\boldsymbol{P}_k^+ = (\boldsymbol{I} - \boldsymbol{K}_k\boldsymbol{C}_a)\boldsymbol{P}_k^- \quad (13)$$

Where Q and R are the covariance matrix of W and V respectively. Q and R are chosen based on the performance of state estimation convergence rate and signal smoothing [11].

2.3 Multiple Sea States Adaptive Algorithm

The block diagram of Multiple-Model Adaptive Estimation (MMAE) is shown in Figure 9. MMAE was first proposed in [20]. The measured outputs, including surge, heave and pitch platform motion signals with noise, are passed to the bank of Kalman Filters model $i = 1, \ldots, M$ which represents different operating points dynamics across the nonlinear dynamics of FOWT. The parallel filters are considered as hypothesis filters, and the one with smallest residual close to the true dynamics.

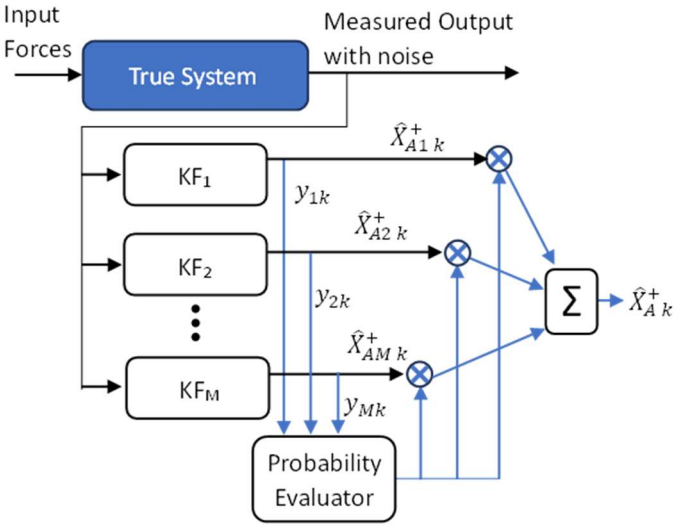

FIGURE 9: MMAE FILTER BLOCK DIAGRAM

The calculation of conditional probability of the i-th model is based on Bayesian theorem. The models are assumed to be stochastic and Gaussian and thus take the form of exponential of negative square of residuals [21]. The weight p of each model and weighted average state value are calculated using:

$$p_{i,k} = \frac{p_{i,k-1}e^{-\frac{1}{2}y_k^T C_f y_k}}{\sum_{i=1}^{M} e^{-\frac{1}{2}y_k^T C_f y_k}\, p_{i,k-1}} \quad (14)$$

$$\hat{\boldsymbol{X}}_{A\,k}^+ = \sum_{i=1}^{M} \hat{\boldsymbol{X}}_{Ai\,k}^+ \cdot p_{i,k} \quad (15)$$

M denotes the number of KF models, C_f is the tuning factor for convergence of probabilities. All the models are initialised by equal probability 1/M. In practice, a lower bound is assigned to prevent the "lock-out" and rejecting of weakly relevant model, and help blending different models for large system[22]. Therefore C_f 0.006 and lower bound 0.1 are chosen.

3. RESULTS AND DISCUSSION

The met-ocean properties of West of Barra, Scotland from LIFES50+ [23] are adopted in this study. In order to generate simulated data for testing the proposed state estimation observer, a time series wave elevation based on sea state 2, 4 and 6 (considered as "unknown") is simulated in QBlade Ocean as shown in Figure 10. While there are 4 preprocessed state dynamic models in the bank of Kalman Filter models corresponding to sea state 1, 3, 5 and 7 for performing the estimation.

The definition of sea states is listed below:

TABLE 1: DEFINITION OF SEA STATES

Sea State (SS) no.	Wave Height *Hs* (m)	Wave Period *Ts* (s)	Remark
1	2	8.93	bank model
2	2.5	9.63	validation
3	3	10.20	bank model
4	3.5	10.68	validation
5	4	11.10	bank model
6	4.5	11.47	validation
7	5	11.80	bank model

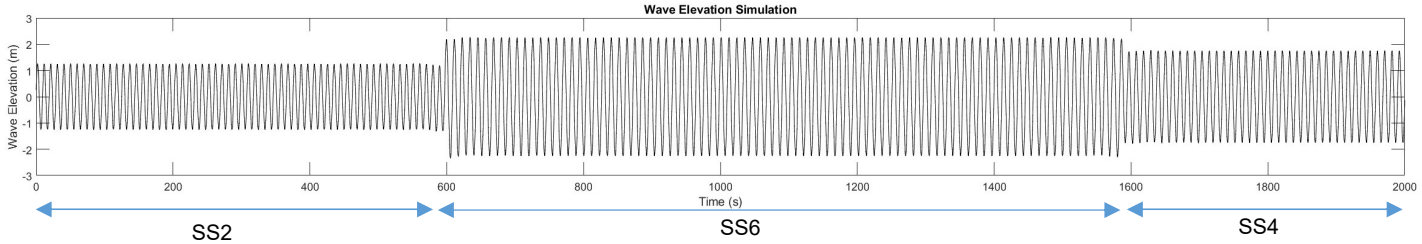

FIGURE 10: SIMULATED "UNKNOWN" SEA STATES WAVE ELEVATION TIME HISTORY

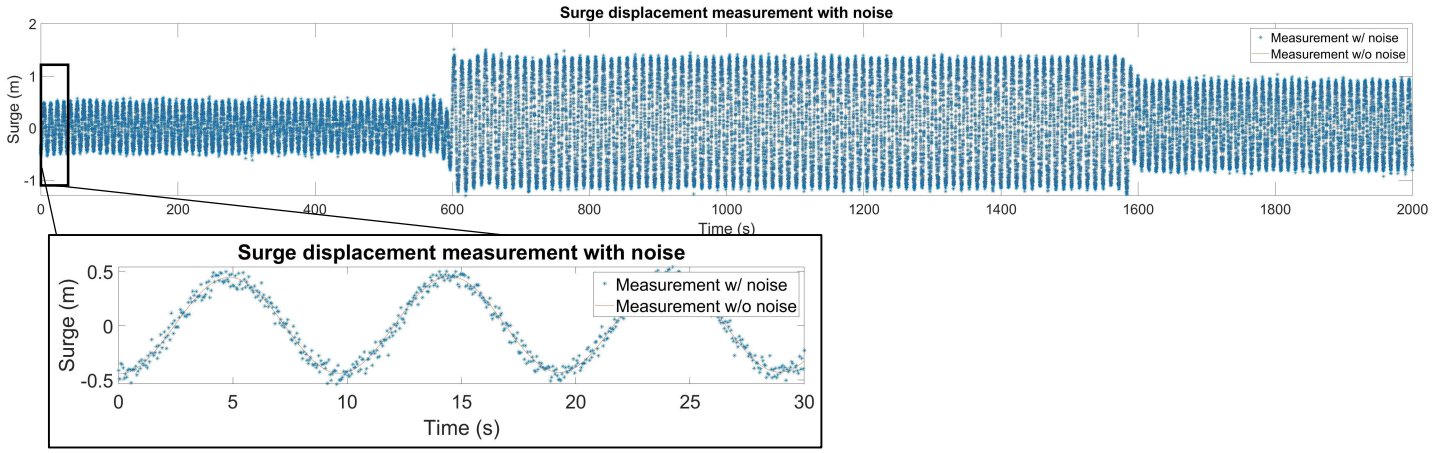

FIGURE 11: SIMULATED MEASUREMENT SIGNAL OF SURGE PLATFORM MOTION WITH NOISE ADDED

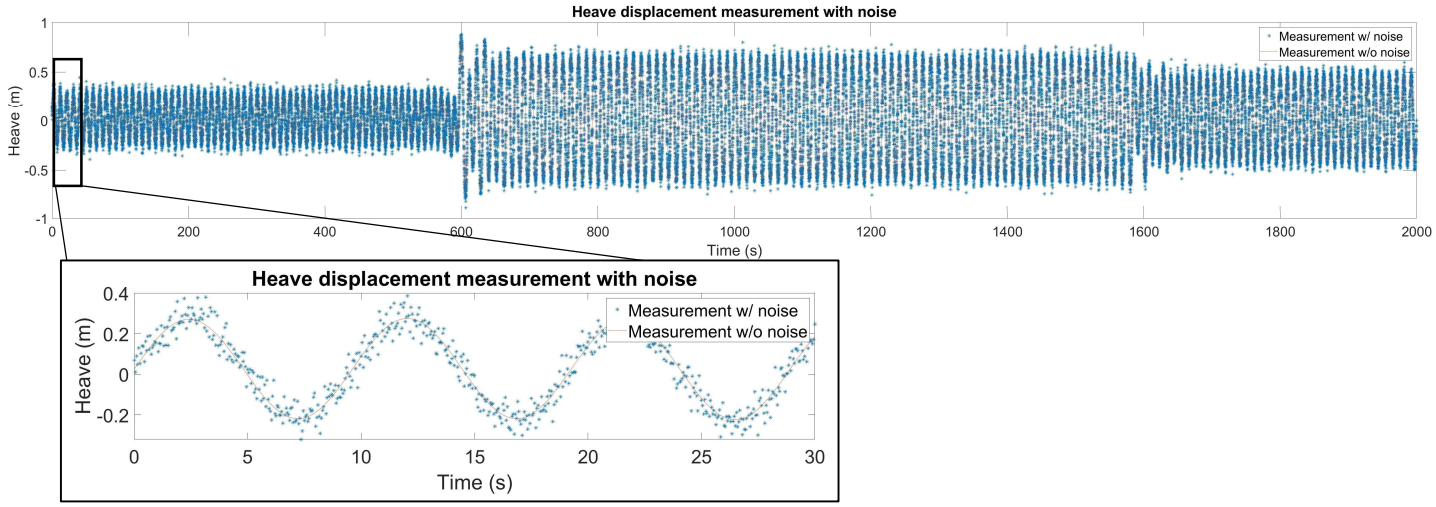

FIGURE 12: SIMULATED MEASUREMENT SIGNAL OF HEAVE PLATFORM MOTION WITH NOISE ADDED

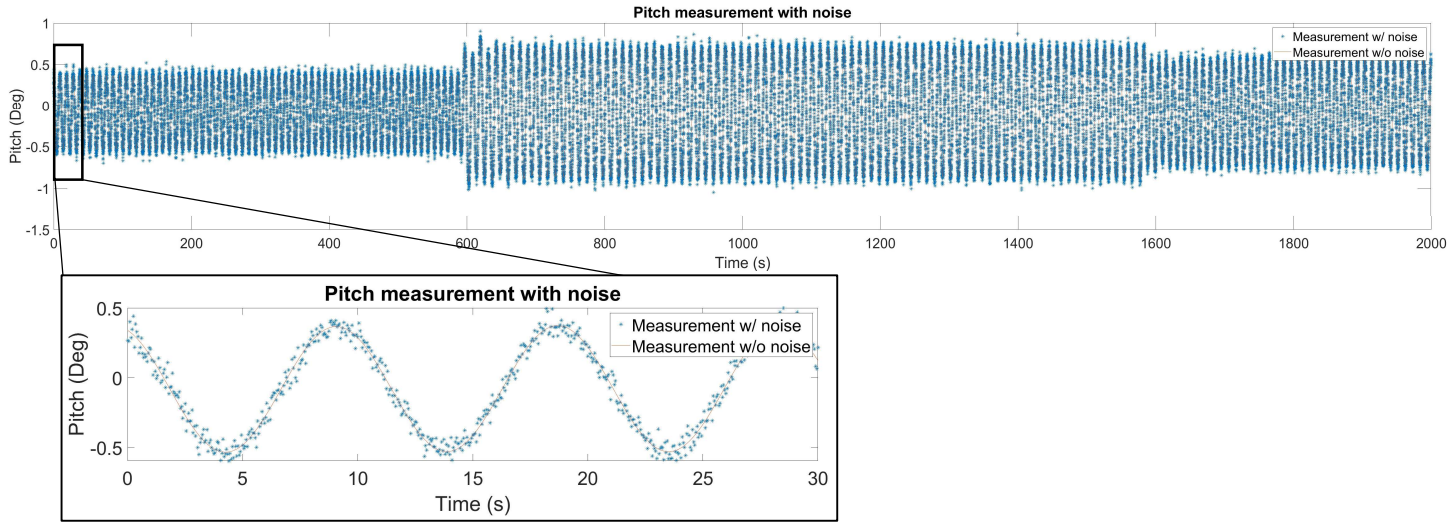

FIGURE 13: SIMULATED MEASUREMENT SIGNAL OF PITCH PLATFORM MOTION WITH NOISE ADDED

A Gaussian noise signal of zero mean and standard deviation of 0.05m Heave, 0.05m Surge and 0.05 degrees Pitch with reference to the accuracy of a typical motion sensor MRU [24] is added to the QBlade simulated measurement signals, as shown in Figure 11, 12 and 13.

The performance is presented with a common metric method of Pearson correlation coefficient defined as

$$\rho = \frac{1}{N-1}\sum_{k}^{N}\left(\frac{X_{est}-\mu_{est}}{\sigma_{est}}\right)\left(\frac{X_{sim}-\mu_{sim}}{\sigma_{sim}}\right)$$

Where μ_{est}, σ_{est} are the mean and standard deviation of estimated value by observer X_{est} , and μ_{sim} and σ_{sim} are the mean and standard deviation of QBlade simulated value X_{sim}, considered N data points.

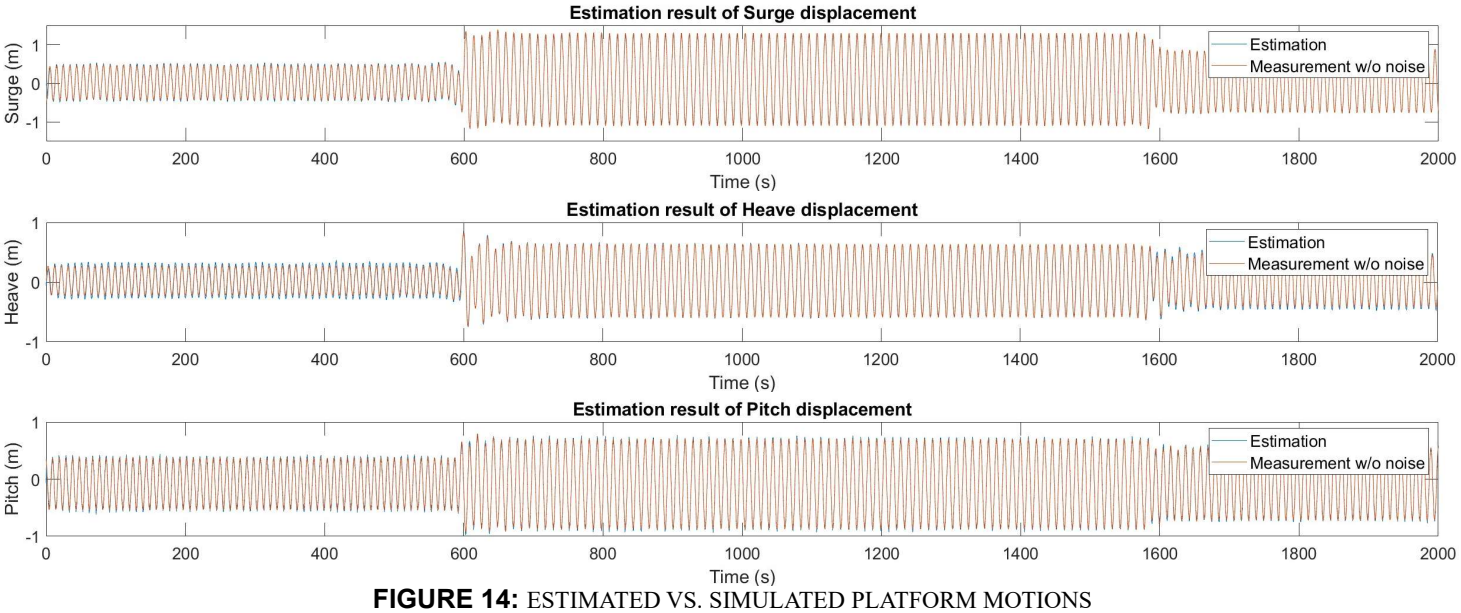

FIGURE 14: ESTIMATED VS. SIMULATED PLATFORM MOTIONS

Figure 14 reveals that the estimated platform motion in surge, heave and pitch are effectively filtered from the sensor noise by the state observer algorithm. Figure 15 shows the results of comparison of estimation from DT prototype and the actual calculated value in QBlade. The phase of cyclic loading and amplitude can be captured by the proposed DT prototype.

TABLE 2: METRIC OF THE PROPOSED ESITIMATOR

	Wave Elevation	Mooring Force in Surge	Mooring Force in Heave	Mooring Force in Pitch
Pearson correlation coefficient	0.9845	0.8136	0.5171	0.9500

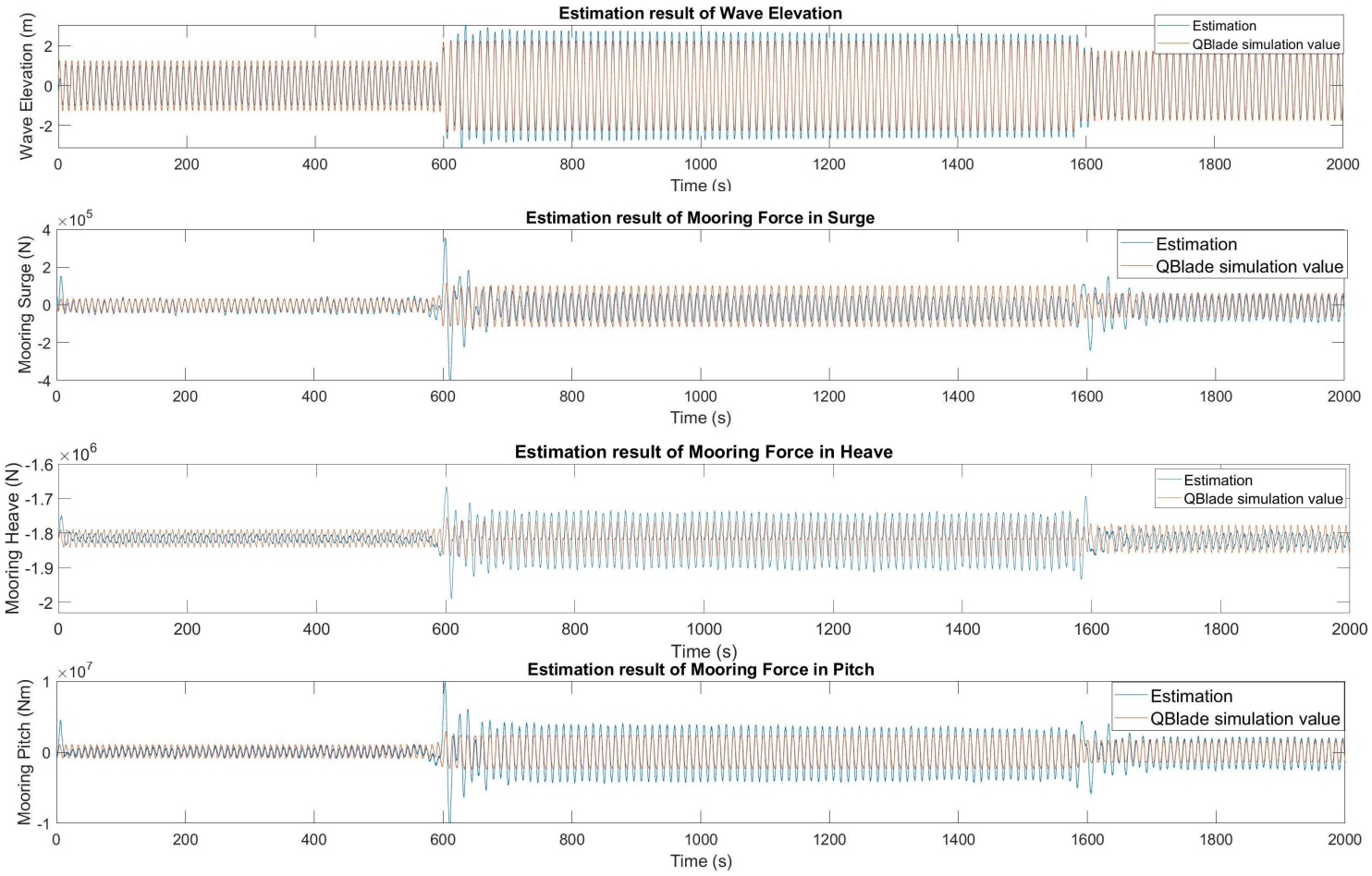

FIGURE 15: ESTIMATED VS. SIMULATED "UNMEASURABLE" STATES, WAVE ELEVATION AND MOORING FORCES

The metric indicates it has strong estimation performance in wave elevation, mooring forces in surge and pitch with more than 0.8. A weaker performance in the estimation of mooring force in heave is due to some phase shifted. The discrepancies of trend and value in between the estimation and simulated true values in Figure 15 are attributed to the limitation of capturing the nonlinear load effect e.g. surge mooring force, and the ability of convergence using linearised Kalman Filter. A detailed stability analysis will be carried out in the future work.

As the observer can be initiated in any arbitrary state value e.g value zero as shown in equation (12), there are some fluctuations at the beginning of estimation and they converge to the optimal values automatically. A larger fluctuation is observed in between the sea state 2 and 6 but it converges effectively to adapt the sudden change in between 2.5m and 4.5m of wave height. This provides an important alert if there is any sudden wave variation in real sea condition, special precaution has to be implemented to protect the structural health of mooring lines. The real-time tracing of cyclic loading pattern can help determine more accurate fatigue life of the mooring line. This eventually reduces the OPEX and the cost spent on inspection. An enhanced estimation of the mooring load through DT can also provide insight of whether the current code of practice requirement underestimates or overestimates the actual value. Consequently, it can optimise the design with lower cost and within the safety factor margin.

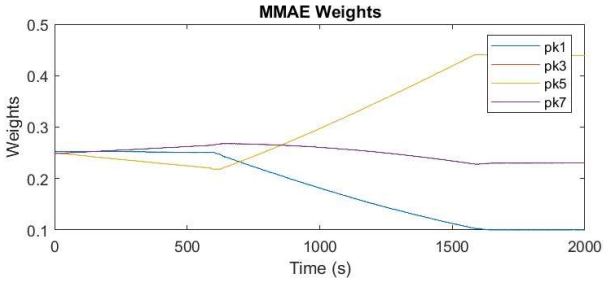

FIGURE 16: VARIATION OF WEIGHTS FOR EACH MODEL

Figure 16 depicts the weights of each Kalman Filter model varying over the simulation time. The pk3 and pk7 have similar and overlapping variation, this indicates model 3 and 7 may have

similar dynamic behaviour. It is observed that the initial sea state 2 can be well blended by the model contribution from 1, 3 and 7, and a clear dominant model 5 is observed during the period of sea state 6. Model 5 continues to have significant contributions for sea state 4 and it has closer dynamic properties than others. As model 1's dynamic is far away from sea state 6 and 4, its contribution declines eventually. The simulation results illustrate that the MMAC scheme can identify the dominant model dynamics and switch to different sea conditions and provide interpolation. This can reduce the number of precomputed bank models and lower the computation cost.

Although limited cases have been examined, in general, this observer can provide valid estimation of the mooring loading with acceptable computation time. The observer algorithm in MATLAB runs on a computer with specification 11th Gen Intel(R) Core (TM) i5-1145G7 @ 2.60GHz 2.61 GHz. Only a time period of about 100 seconds is required to perform estimation for a 2000 seconds data set.

4. CONCLUSION

It is demonstrated that the PM approach is valid for some weak nonlinear scenarios as discussed in this paper. This work provides an important foundation for the new DT, especially estimating the difficult measurable states mooring forces and wave elevations based on only the platform motions. In addition, this new approach can avoid possible problems with underwater sensors' fragility and save extremely high cost of doing their repairment. The estimated total restoring force can be further analysed to reconstruct the local stress analysis in Finite Element Modeling. The predicted wave elevation can be further analysed for forecasting and to improve the controller of FOWT.

In this paper, only a preliminary prototype of DT is presented and the environmental loading case is simplified. In order to achieve better DT, the future work might include different loading combinations e.g. wind, wave and current and a wider spectrum of sea states. The linear time-invariant model of Discrete Kalman Filter may not be able to capture the highly non-linear wave properties in real condition, a more advanced Unscented Kalman Filter is required.

ACKNOWLEDGEMENTS

The author would like to thank the John Anderson Research Award PhD scholarship granted by University of Strathclyde and the financial support from Ove Arup & Partners Hong Kong Ltd. The author would also like to acknowledge the technical advice from Mr Xiang Li, a member of Prof Xiao's research group.

REFERENCES

[1] Crown Estate, Offshore Wind Report 2021
[2] European Union (EU), "Mooring System Integrity Management through Monitoring, Digital Twin and Control Technologies for Cost Reduction and Increased Efficiency", 2020
[3] ABSG Consulting INC., "Study on Mooring System Integrity Management for Floating Structures," 2015.
[4] J. Minnebo, P. Aalberts and A. Duggal, "Mooring system monitoring using DGPS," Proceedings of the International Conference on Offshore Mechanics and Arctic Engineering - OMAE, vol. 1B, 2014.
[5] "Mooring System Engineering for Offshore Structures. Chapter 12 - Inspection and monitoring". Kai-Tung Ma, Yong Luo, Thomas Kwan, Yongyan Wu. 2019
[6] Walker, J., Coraddu, A., Collu, M. et al. Digital twins of the mooring line tension for floating offshore wind turbines to improve monitoring, lifespan, and safety. J. Ocean Eng. Mar. Energy 8, 1–16 (2022). https://doi.org/10.1007/s40722-021-00213-y
[7] Li CB, Choung J, Noh MH, Wide-banded fatigue damage evaluation of Catenary mooring lines using various Artificial Neural Networks models. Mar Struct 60:186–200 (2018)
[8] Yao, J., Wu, W. and Li, S. 'Anomaly detection model of mooring system based on LSTM PCA method', Ocean Engineering, 254 (2022), p. 111350. doi:10.1016/j.oceaneng.2022.111350.
[9] Willmott CJ, Matsuura K Advantages of the mean absolute error (MAE) over the root mean square error (RMSE) in assessing average model performance. Clim Res 30(1):79–82 (2005)
[10] J. Gumley, M. Henry and A. Potts, "A novel method for predicting the motion of moored floating bodies," in ASME 2016 35th International Conference on Ocean, Offshore and Arctic Engineering-OMAE, 2016.
[11] D. Simon, "Optimal State Estimation: Kalman, H Infinity, and Nonlinear Approaches," John Wiley & Sons, Hobo- ken, 2006
[12] Branlard, E., Jonkman, J., Brown, C., and Zang, J.: A digital-twin solution for floating offshore wind turbines validated using a full-scale prototype, Wind Energ. Sci. Discuss. [preprint], https://doi.org/10.5194/wes-2023-50, in review, 2023.
[13] Marten, D.: Qblade Website (2022), http://www.q-blade.org
[14] Robertson, A., Jonkman, J., Masciola, M., Song, H., Goupee, A., Coulling, A., & Luan, C. Definition of the Semisubmersible Floating System for Phase II of OC4. United States
[15] F. Papi, A. Bianchini, G. Troise, G. M. Mirra, D. Marten, J. Saverin, R. B. de Luna, M. L. Ducasse, J. Honnet, 2022, "FLOATECH D2.4 Full report on the estimated reduction of uncertainty in comparison to the state-of-the-art codes OpenFAST and DeepLines Wind™", FLOATECH Deliverable 2.4, Technical Report
[16] J.M.J. Journée and W.W. Massie, "Offshore Hydromechanics", First Edition, January 2001, Delft University of Technology
[17] Wiley, W., Jonkman, J., Robertson, A., and Shaler, K.: Sensitivity Analysis of Numerical Modeling Input Parameters on Floating Offshore Wind Turbine Loads, Wind Energ. Sci. Discuss. [preprint], https://doi.org/10.5194/wes-2023-49, in review, 2023.

[18] Ljung, L. System Identification: Theory for the User, Appendix 4A, Second Edition, pp. 132–134. Upper Saddle River, NJ: Prentice Hall PTR, 1999.
[19] Zarchan, Paul Musoff, Howard. Fundamentals of Kalman Filtering - A Practical Approach (4th Edition) - Progress in Astronautics and Aeronautics, Volume 246. American Institute of Aeronautics and Astronautics/Aerospace Press (AIAA). (2015).
[20] D. Magill, “Optimal adaptive estimation of sampled stochastic processes,” IEEE Trans. on Automat. Contr., vol. 10, pp. 434–439, 1965.
[21] R. Rao, B. Aufderheide, and B. Bequette, “Experimental studies on multiple-model predictive control for automated regulation of hemo-dynamic variables,” IEEE Trans. Biomed. Eng., vol. 50, pp.
[22] P. Eide and P. Maybeck, "An MMAE failure detection system for the F-16," in IEEE Transactions on Aerospace and Electronic Systems, vol. 32, no. 3, pp. 1125-1136, July 1996, doi: 10.1109/7.532271.
[23] European Union (EU), “Deliverable 1.1 Oceanographic and meteorological conditions for the design”
[24] Motion sensor Forsberg Services Ltd. https://www.nauticexpo.com/prod/inertial-labs-inc/product-195447-562308.html